



**HAL**  
open science

## Heterodimerization with Jun Family Members Regulates c-Fos Nucleocytoplasmic Traffic

Cécile Malnou, Tamara Salem, Frederique Brockly, Harald Wodrich, Marc Piechaczyk, Isabelle Jariel-Encontre

► **To cite this version:**

Cécile Malnou, Tamara Salem, Frederique Brockly, Harald Wodrich, Marc Piechaczyk, et al.. Heterodimerization with Jun Family Members Regulates c-Fos Nucleocytoplasmic Traffic. *Journal of Biological Chemistry*, 2007, 282 (42), pp.31046-31059. 10.1074/jbc.M702833200 . hal-02384505

**HAL Id: hal-02384505**

**<https://hal.umontpellier.fr/hal-02384505>**

Submitted on 27 May 2021

**HAL** is a multi-disciplinary open access archive for the deposit and dissemination of scientific research documents, whether they are published or not. The documents may come from teaching and research institutions in France or abroad, or from public or private research centers.

L'archive ouverte pluridisciplinaire **HAL**, est destinée au dépôt et à la diffusion de documents scientifiques de niveau recherche, publiés ou non, émanant des établissements d'enseignement et de recherche français ou étrangers, des laboratoires publics ou privés.



Distributed under a Creative Commons Attribution 4.0 International License

# Heterodimerization with Jun Family Members Regulates c-Fos Nucleocytoplasmic Traffic\*

Received for publication, April 3, 2007, and in revised form, July 31, 2007 Published, JBC Papers in Press, August 6, 2007, DOI 10.1074/jbc.M702833200

Cécile E. Malnou<sup>1</sup>, Tamara Salem, Frédérique Brockly, Harald Wodrich, Marc Piechaczyk<sup>2</sup>, and Isabelle Jariel-Encontre<sup>3</sup>

From the Institut de Génétique Moléculaire de Montpellier, CNRS, UMR5535, 1919 Route de Mende, Montpellier F-34293, France

c-Fos proto-oncoprotein forms AP-1 transcription complexes with heterodimerization partners such as c-Jun, JunB, and JunD. Thereby, it controls essential cell functions and exerts tumorigenic actions. The dynamics of c-Fos intracellular distribution is poorly understood. Hence, we have combined genetic, cell biology, and microscopic approaches to investigate this issue. In addition to a previously characterized basic nuclear localization signal (NLS) located within the central DNA-binding domain, we identified a second NLS within the c-Fos N-terminal region. This NLS is non-classic and its activity depends on transportin 1 *in vivo*. Under conditions of prominent nuclear localization, c-Fos can undergo nucleocytoplasmic shuttling through an active Crm-1 exportin-independent mechanism. Dimerization with the Jun proteins inhibits c-Fos nuclear exit. The strongest effect is observed with c-Jun probably in accordance with the relative stabilities of the different c-Fos:Jun dimers. Retrotransport inhibition is not caused by binding of dimers to DNA and, therefore, is not induced by indirect effects linked to activation of c-Fos target genes. Monomeric, but not dimeric, Jun proteins also shuttle actively. Thus, our work unveils a novel regulation operating on AP-1 by demonstrating that dimerization is crucial, not only for active transcription complex formation, but also for keeping them in the compartment where they exert their transcriptional function.

The dimeric transcription factors of the AP-1 family control virtually all cell fates. They play essential roles in most major physiological processes and are involved in various pathological situations, including tumorigenesis (for reviews see Refs. 1–5). Consistently, AP-1 is controlled by a plethora of physiological stimuli and environmental insults operating at multiple transcriptional, post-transcriptional, and post-translational levels to prevent deleterious expression and/or activity.

The best-studied AP-1 components are the Fos (c-Fos, FosB,

Fra-1, and Fra2) and Jun (c-Jun, JunB, and JunD) proteins that dimerize via a leucine zipper (LZ)<sup>4</sup> domain and recognize their target DNA sequences owing to an adjacent, upstream basic DNA-binding domain (DBD) (6). In contrast to the Jun family members, Fos proteins cannot homodimerize. They must heterodimerize with different partners, including the Jun proteins, to form active AP-1 dimers.

c-Fos (for a review, see Ref. 7) is expressed constitutively in diverse primary tumors and cancer cell lines (3) and in certain tissues *in vivo*. In most other cells, it can be rapidly and transiently induced by many stimuli, including mitogens, cytokines, hormones, and stresses (4), to convert them into long-term responses the nature of which depends on the cell context and the stimulus. Not only the multiplicity of its dimerization partners is important for c-Fos specificity and activity, but also the many post-translational modifications it is subjected to. Thus, c-Fos is an unstable protein undergoing proteasome-dependent degradation (8–11). Proteolysis of the bulk of c-Fos is essentially ubiquitylation-independent (12), which is also the case for its Fra-1 relative (13), but can under certain conditions involve ubiquitylation (14). Moreover, c-Fos transcriptional activity, which depends on multiple transactivation domains, is stimulated upon phosphorylation of various threonines in response to either oncogenic Ras GTPases or kinases of the Erk1/2 MAPK kinase pathway (for a review, see Ref. 15). By contrast, it is reduced upon sumoylation at a unique lysine (16).

One aspect of c-Fos biology that has been poorly studied is the control of intracellular localization. Usually, the protein predominantly accumulates within the nucleus (17, 18). Entry into the nucleus does not require prior LZ-dependent heterodimerization but likely depends on at least two nuclear localization signals (NLS) (18, 19). Thus far, only one NLS has been characterized in details. It consists of an arginine-rich basic motif residing within the DBD (amino acids 139–160) (18). c-Fos displays high *in vitro* affinity for importin  $\beta$  1 (Imp $\beta$ 1) (20), a member of the importin  $\beta$  superfamily of nuclear transport receptors that recruit protein cargoes within

\* This work was supported in part by grants from the Association pour la Recherche sur le Cancer and the Action Concertée Incitative Biologie Cellulaire of the French Ministry of Research. The costs of publication of this article were defrayed in part by the payment of page charges. This article must therefore be hereby marked "advertisement" in accordance with 18 U.S.C. Section 1734 solely to indicate this fact.

<sup>1</sup> Supported by a fellowship from the Association pour la Recherche sur le Cancer.

<sup>2</sup> M. P.'s laboratory is an Equipe labellisée of the French Ligue Nationale contre le Cancer. To whom correspondence may be addressed: Tel.: 33-4-67-61-36-68; Fax: 33-4-67-04-02-31; E-mail: marc.piechaczyk@igmm.cnrs.fr.

<sup>3</sup> To whom correspondence may be addressed: Tel.: 33-4-67-61-36-68; Fax: 33-4-67-04-02-31; E-mail: isabelle.jariel@igmm.cnrs.fr.

<sup>4</sup> The abbreviations used are: LZ, leucine zipper; DBD, DNA-binding domain; MAPK, mitogen-activated protein kinase; Erk, extracellular signal-regulated kinase; NLS, nuclear localization signal; TRN1, transportin 1; GFP, green fluorescent protein; EGFP, enhanced GFP; GST, glutathione S-transferase; YFP, yellow fluorescent protein; NES, nuclear export signal; HA, hemagglutinin; CHX, cycloheximide; PEG, polyethylene glycol; LMB, leptomycin B; PBS, phosphate-buffered saline; siRNA, small interference RNA; Imp $\beta$ 1, importin  $\beta$ 1; STAT3, signal transducers and activators of transcription 3; FRAP, fluorescence recovery after photobleaching; FLIP, fluorescence loss induced after photobleaching; BiFC, bimolecular fluorescence complementation.

the cytoplasm, address them to the nucleopore complex, and mediate their translocation through the nucleopore complex (21, 22). More recently, a digitonin-permeabilized cell-based *in vitro* assay suggested that c-Fos nuclear transport may rather involve two importins, one being Imp $\beta$ 1, through interaction with the basic NLS, the other being transportin 1 (TRN1), interacting with an unidentified upstream NLS (23). In this biochemical assay, the TNR1- and Imp $\beta$ 1-dependent pathways showed mutual exclusion with TNR1 appearing more efficient for c-Fos nuclear import.

c-Fos is also found cytoplasmic in various situations. Its transport into the nucleus depends on extra- and intracellular signals that may be absent depending on the conditions. Thus, in cells constitutively expressing it, c-Fos progressively becomes exclusively cytoplasmic within a few hours upon removal of serum from the culture medium (17, 24). Preferential cytoplasmic localization associated with faster turnover is also observed when endogenous c-Fos is induced by STAT3 signaling under conditions where the Erk5 kinase pathway is inactivated (14). This intracellular redistribution seems to depend, at least in part, on c-Fos nuclear export by the Crm-1 exportin (14). Furthermore, a fraction of c-Fos associates with the endoplasmic reticulum to activate phospholipid metabolism in a transcription activity-independent manner (25). This appears to be required for neurite elongation (26), suggesting a physiological cytoplasmic role for c-Fos in addition to its long known nuclear one in transcription. Finally, cytoplasmic retention of c-Fos is reversed upon activation of cAMP-dependent protein kinase A (17) and upon that of p38 MAPKs by UV irradiation (27).

The afore-mentioned observations suggest that actively regulated nucleocytoplasmic traffic may contribute to c-Fos activity regulation. We have therefore combined genetic, cell biology, and microscopic studies to investigate c-Fos nucleocytoplasmic shuttling, including when the protein is essentially nuclear, to characterize more precisely c-Fos second NLS and to assess the actual roles of Imp $\beta$ 1 and TRN1 in its nuclear import *in vivo*.

## EXPERIMENTAL PROCEDURES

**Plasmids, Cloning, and Mutagenesis**—Cloning and mutagenesis were performed using standard PCR-based methods into the cytomegalovirus promoter-based pcDNA3 expression vector (Invitrogen). The c-Fos open reading frame was from rat, and those of Jun proteins were from mouse. EGFP chimeras were constructed using the pEGFP-C1 or the pEGFP-N1 vectors from Clontech. The GST open reading frame was recovered from pGEX-2T plasmid (Amersham Biosciences). YFP-based plasmids for bi-molecular fluorescence complementation (BiFC) experiments are described in Hu *et al.* (28). YFP-(1–154) was connected to c-Fos using the RSIAT linker and YFP-(155–238) to c-Jun and JunB using the RPACK-IPNDLKQKVMNH peptide. pDsRed2-C1 and pDsRed-m-C1 were from Clontech. Mouse c-Jun-FLAG (29), JunD-FLAG (30), HA-HDAC4 (31), and the tethered c-Jun~c-Fos dimer expression plasmid (32) are cytomegalovirus promoter-based vectors. JunB-FLAG was cloned in the cytomegalovirus promoter-based pcDNA3 vector. GST/NLS/GFP and GST/NLS/

GFP/NES open reading frames were recovered from pR1GsvNLSF1 and pR1GsvNLSFrevNES1 (33), respectively, and cloned into pcDNA3.

**Antibodies**—c-Fos was immunodetected using the sc52 rabbit, the sc52 goat, or the H125 rabbit antisera. c-Jun was detected with the sc45, JunB with the sc46, JunD with the sc74, and TRN1 with the sc6914 rabbit antisera. All the afore-mentioned antibodies were from Santa Cruz Biotechnology (Santa Cruz, CA). HA- and FLAG-tagged proteins were detected using the 3F10 rat monoclonal anti-HA (Sigma) and the mouse monoclonal M2 anti-FLAG (Roche Applied Science) antibodies, respectively. Rabbit anti-exportin7, anti-importin7, and anti-TRN2 antibodies were kind gifts from Drs D. Görlich and U. Kutay. The secondary fluorescein isothiocyanate-labeled and horseradish peroxidase-conjugated antibodies were from Sigma, and the secondary Alexa647- and Alexa488-labeled antibodies were from Molecular Probes. Immunoprecipitations were performed using the M2 anti-FLAG antibody coupled to protein A-agarose.

**Chemicals**—Hoescht 33342, cycloheximide (CHX), Hybrimax polyethylene glycol (PEG), and leptomycin B (LMB) were from Sigma. Paraformaldehyde was from Electron Microscopy Sciences, Permafluor from Shandon Immunon, and complete mini protease inhibitor mixture tablets from Roche Applied Science. CHX and LMB were used at final concentrations of 50  $\mu$ g/ml and 20 to 100 nM, respectively.

**Cells, Culture, and Transfection**—Mouse BALB/c 3T3 fibroblasts and human HeLa cells are available from the ATCC and were grown under standard conditions. The f10 c-fos<sup>-/-</sup> mouse embryo fibroblast cell line (34) is a kind gift from E. Wagner. Transfections were performed using the calcium phosphate coprecipitation procedure (35). Transfections were routinely carried out using 3  $\mu$ g of plasmid per 10<sup>6</sup> cells. When necessary, 3  $\mu$ g of pDsRed2 or pDsRed-m-C1 were also co-transfected. Transfection time was limited to 16 h to avoid overexpression, except for BiFC experiments where cells were incubated for another 8 h at 30 °C before PEG-mediated fusion to allow for optimal renaturation of YFP.

**Heterokaryon Experiments**—Heterokaryon assays were essentially performed as described by Roth *et al.* (36) using cells seeded on glass coverslips. To investigate endogenous c-Fos protein nucleocytoplasmic shuttling, BALB/c 3T3 cells were serum-deprived for 48 h and, then, stimulated by addition of fresh medium containing 20% serum. 1 h later, freshly trypsinized HeLa cells, previously transfected with the pDsRed2-C1 plasmid for 16 h, were added in the presence of CHX. After another 2 h, *i.e.* time sufficient for cell spreading, coverslips were quickly rinsed in PBS (150 mM NaCl, 10 mM sodium phosphate, pH 7), covered with a 50% w/v solution of PEG for 2 min, again carefully washed with PBS, and, finally, incubated at 37 °C for 1 h in fresh medium containing 10% serum and CHX. Cells were then fixed and treated for microscopic examination. To study shuttling efficiency at low temperature, HeLa cells transfected with appropriate expression plasmids were PEG-fused with BALB/c 3T3 cells, let at 37 °C for 15 min to allow completion of heterokaryon formation, and, then, placed on ice for 45 min before cell fixation and microscope analysis. To study EGFP-c-Fos and EGFP-c-Fos $\Delta$ LZ

## c-Fos Nucleocytoplasmic Traffic

shuttling during the  $G_0/G_1$  transition, f10 *c-fos*<sup>-/-</sup> mouse embryo fibroblasts were stably transfected with expression plasmids for each one of the two proteins under the transcriptional control of a minimal *c-fos* promoter containing the serum-responsive element and recapitulating the transient induction of normal *c-fos* gene (9, 10, 12, 13). Transfectants were starved for 36 h, trypsinized, stimulated by resuspension in fresh culture medium containing 20% serum, and placed over a monolayer culture of asynchronous HeLa cells grown on coverslips. One hour later, *i.e.* a time sufficient for transfectant attachment, cells were PEG-fused and let for another 1 h at 37 °C in presence of CHX before fixing and direct fluorescence microscopy analysis. For analysis of ectopic wild-type and mutant c-Fos and c-Jun proteins as well as that of EGFP chimeras, HeLa cells were co-transfected with pDsRed2-C1 and the relevant expression vector(s). 16 h later, freshly trypsinized BALB/c 3T3 cells were added in the presence of CHX, with or without LMB, for 2 h. Fusion was performed as above, and cells were incubated at 37 °C for another 1 h in the presence of LMB, when needed, before treatment for microscopic examination.

**Localization of c-Fos at Low Temperature**—For the analysis of c-Fos redistribution at low temperature, HeLa cells were transfected with expression vectors for either EGFP/NLS/NLS or c-Fos and, 16 h later, placed on ice for 1 h before fixation and microscopic analysis.

**Immunofluorescence**—Cells were fixed in 4% paraformaldehyde at room temperature for 30 min, washed twice in PBS, permeabilized with 0.2% Triton X-100 at room temperature for 5 min, and, then, washed twice in PBS before incubation in PBS containing 0.5% bovine serum albumin for 15 min. Protein immunodetections were carried out with optimized dilutions of primary- and fluorescein isothiocyanate-, Alexa488-, and Alexa647-conjugated secondary antibodies. Nuclei were stained using Hoescht 33342 at a 0.2 µg/ml concentration for 5 min. Coverslips were mounted in Permafluor. Observations were performed using either a Leica DMRA microscope equipped with a 63× oil lens and a coolsnap FX camera or a confocal Leica DMR microscope equipped with a 63× oil lens, a confocal spinning disc (Yokogawa), and a coolsnap FX camera. Fluorescence signal quantifications were performed using the Metamorph software and 12-bit images.

**FRAP and FLIP Experiments**—FRAP and FLIP analysis were performed at 37 °C with a Zeiss LSM510 Meta microscope equipped with a heating chamber and a plan Apochromat 63× water immersion lens. For EGFP fluorescence monitoring, cells were excited with an argon laser at a wavelength of 488 nm, and emission was collected using the 505–550 nm wavelength bandpass filter. For DsRed2-monomer fluorescence monitoring, cells were excited with the 543 nm wavelength laser, and emission was collected using the 560 nm wavelength long path filter. Before photobleaching, five fluorescence intensity measurements were made over a period of 5 min. For FRAP experiments, HeLa cells were washed once with PBS, incubated with PEG for 1 min, washed again 10 times with PBS to remove any trace of PEG and incubated at 37 °C in Dulbecco's modified Eagles medium containing 10% serum. One hour later, cells were co-transfected with pDsRed-m-C1 and the plasmid of interest. 19 h after fusion, FRAP experiments were carried out

on cells previously cultured in the presence of CHX for 1 h. Photobleaching was carried out on the whole surface of one targeted nucleus of the homopolykaryon using the 488 nm wavelength laser at maximal power. The bleach was of 256 µs/pixel. The recovery of fluorescence in the bleached area was monitored every minute. For FLIP experiments, HeLa cells were co-transfected with the pDsRed-m-C1 for visualization of the cytoplasm and the plasmid of interest. 16 h later, approximately half of the cytoplasm of the transfected cells was irradiated every minute for 10–15 s with the 488 nm wavelength laser at maximal power with a bleach of 25.6 µs/pixel. Nuclear fluorescence was monitored after each bleach.

**siRNA Experiments**—siRNAs against Impβ1 (sc35736) and TRN1 (sc35737) were purchased from Santa Cruz Biotechnology. The anti-TRN2 siRNA, which was a mix of two sequences (5'-GUGGCCUCAUCCUCAAGAATT-3' and 5'-GCAGUUCUCUGAGCAAUUCTT-3') and the anti-Imp7 (5'-GAUGGAGCCCUGCAUAUGA-3') siRNA were purchased from Eurogentec. They (200 pmol/well) were transfected in HeLa cells ( $3 \times 10^5$  cells/well of 6-well plates) using Oligofectamine (3 µl/well) according to the supplier (Invitrogen) specifications. Thirty-six hours later, cells were transfected with the plasmids of interest using the calcium phosphate coprecipitation procedure (3 µg of plasmid per 35-mm culture dish). 16 h later, they were fixed for microscopic observation or lysed in the RIPA buffer (50 mM Tris-HCl, pH 8.0, 150 mM NaCl, 0.02% NaN<sub>3</sub>, 0.1% SDS, 1% Nonidet P-40, 0.5% deoxycholic acid sodium salt, 1 Complete Mini protease inhibitor mixture tablet per 10-ml buffer) for immunoblotting analysis.

**Immunoprecipitation and Immunoblotting Assays**—Immunoprecipitations were performed as in a previous study (16).  $10^7$  cells were lysed in 600 µl of radioimmune precipitation assay buffer. To immunoprecipitate FLAG-tagged proteins, 200 µl of lysates was incubated with 30 µl of anti-FLAG M2 affinity gel (Sigma) for 3 h. Lysates were then centrifuged, supernatants were collected, and pellets were resuspended in Laemmli electrophoresis loading buffer after five washes. Total extracts, supernatants, and immunoprecipitated fractions were then submitted to immunoblotting analysis. For this, proteins were electrotransferred on polyvinylidene difluoride membranes after fractionation through 12% PAGE-SDS gels. Immunoblots were probed with the appropriate antibodies. Quantification of luminescence signals was performed using the GeneGnome system from Syngene.

**Cell Fractionation Experiments**—Cell fractionation experiments were performed as previously described in (37). Briefly,  $10^7$  cells were scrapped in PBS on ice, harvested by low speed centrifugation, and resuspended in 200 µl of cold buffer A (10 mM Hepes, pH 7.9, 10 mM KCl, 1.5 mM MgCl<sub>2</sub>, 0.34 M sucrose, 10% glycerol, 1 mM dithiothreitol, 1 Complete Mini protease inhibitor mixture tablet per 10 ml of buffer). Cells were then lysed on ice for 15 min by addition of 0.15% Triton X-100 and centrifuged at 3500 rpm at 4 °C for 5 min. The supernatants (S) contained both the cytoplasmic and the nuclear soluble fractions. Nuclei were then washed once in 200 µl of cold buffer B (3 mM EDTA, 0.2 mM EDTA, 1 mM dithiothreitol, and the Complete Mini protease inhibitor mixture) and centrifuged. The centrifugation supernatants corresponded to the wash fraction

(W). The pellets (P) corresponding to the nonsoluble fraction were directly resuspended in denaturing Laemmli electrophoresis loading buffer. Equivalent amounts of the three fractions were then submitted to immunoblotting analysis. An anti-Phax monoclonal antibody (monoclonal antibody 8G5, gift of Dr. E. Bertrand) was used to characterize the soluble nuclear fraction, and an anti-topoisomerase I one (gift of Dr. J. Tazi) was used to characterize the insoluble one (see Ref. 16).

## RESULTS

*c-Fos Shuttles between the Nucleus and the Cytoplasm*—We first tested the nucleocytoplasmic shuttling activity of c-Fos under conditions of prominently nuclear steady-state localization. This was achieved in classic heterokaryon assays in which a donor cell expressing the protein of interest is fused to an acceptor cell not expressing it in the presence of PEG. The experiment was performed in the presence of CHX to prevent bias possibly generated by newly synthesized proteins. In case of shuttling, the studied protein is reimported indifferently in both donor and acceptor cell nuclei, after exit from the donor nucleus.

Transient induction by growth factors in cells re-entering the cell cycle is one of the best-characterized physiological situations to study c-Fos. Therefore, quiescent BALB/c 3T3 mouse embryo fibroblasts were stimulated by serum to induce endogenous c-Fos whose transient expression peaks by 1–2 h post-stimulation and returns to basal level 4–6 h later when cells traverse the G<sub>0</sub>/G<sub>1</sub> transition (38). They were then fused to asynchronous human HeLa cells expressing an ectopic red fluorescent protein (Ds-Red) for visualization of heterokaryons. c-Fos distribution was monitored by indirect immunofluorescence 1 h post fusion, DNA staining with Hoechst 33342 permitting easy discrimination of human and mouse nuclei. Fig. 1A (*panel a*) shows a clear accumulation of c-Fos in human acceptor nuclei. Similar results were obtained in the reverse experiment when serum-stimulated HeLa cells were used as donors and BALB/c fibroblasts as acceptors (not shown). Thus, endogenous c-Fos can shuttle under physiological conditions of expression.

We then expressed an exogenous c-Fos in asynchronous HeLa cells, which is a situation mimicking constitutive nuclear expression found in certain tissues and tumors, and investigated c-Fos shuttling activity. To avoid biases linked to overexpression, transfection was optimized to ensure a c-Fos accumulation level comparable to that of the endogenous protein induced by serum stimulation (not shown). One hour post fusion with asynchronous BALB/c fibroblasts, c-Fos was found in both human and mouse nuclei of heterokaryons (Fig. 1A, *panel b*), indicating ability to shuttle in this setting. Heterokaryon formation is not synchronous but spread over time following PEG treatment, which makes impossible to precisely measure the half-time for c-Fos return to the cytoplasm. However, quantification of c-Fos transfer from HeLa to BALB/c cell nuclei allowed to estimate c-Fos half-return time to the cytoplasm to be <30 min. This value is much less than the 2.5 h half-life of c-Fos in exponentially growing BALB/c and HeLa cells (10, 12) indicating the possibility for c-Fos to undergo several rounds of nucleocytoplasmic shuttling during its lifespan.

Heterokaryon assays may lead to misinterpretation on actual physiological protein shuttling ability, because PEG also induces transient endoplasmic reticulum disruption (39), which results in release of calreticulin that can operate as an illegitimate exportin for ~1 h (39). To exclude this possibility for c-Fos, we first used a fluorescence recovery after photobleaching (FRAP) approach. Because these experiments on living cells required the use of fluorescent proteins, we resorted to a chimera (EGFP/c-Fos) in which c-Fos was C-terminally fused to enhanced green fluorescent protein (EGFP). Previous work (10) has shown that, in contrast to EGFP, which diffuses freely within the whole cell due to its small size and absence of both NLS and nuclear export signal (NES), EGFP/c-Fos displays the typical nuclear localization with nucleolar exclusion of c-Fos (see Fig. 4). Moreover, this chimera keeps other properties such as transcriptional activation of an AP-1-dependent reporter gene and Erk1/2 pathway-inhibitable proteasomal degradation, which validates its use in a number of settings. Homopolykaryons formed of PEG-fused HeLa cells were transfected to express EGFP/c-Fos. Twenty hours later, *i.e.* a time much longer than that sufficient for endoplasmic reticulum restoration (39), one of the EGFP/c-Fos-positive homopolykaryon nuclei was photobleached after protein synthesis arrest by CHX. Recovery of nuclear fluorescence, due to entry of EGFP/c-Fos originating from the non-FRAPped nuclei, was monitored as a function of time. A typical experiment is presented in Fig. 1B (*panels a* and *c*). Progressive recovery of the fluorescence in the bleached nucleus correlated with a concomitant and proportional decrease of fluorescence in the non-bleached nucleus of a homodikaryon and fluorescence equilibrium between the two nuclei was reached by 2 h. This process was specific because no, or very low, fluorescence recovery was observed 2 h post-bleach when a control non-shuttling GST/NLS/GFP protein made up of GST, NLS of the SV40 virus LT antigen, and GFP (33) was analyzed (Fig. 1B, *panels b* and *d*).

Next, a fluorescence loss induced after photobleaching (FLIP) assay further demonstrated that membrane fusion was not responsible for induction of c-Fos nuclear export and excluded bias possibly due to protein synthesis inhibition as outcomes were identical whether CHX was present or not. Individual HeLa cells expressing either the non-shuttling nuclear GST/NLS/GFP, as a negative control, or EGFP chimeras with C-terminal (EGFP/c-Fos) or N-terminal (c-Fos/EGFP) c-Fos extensions were photobleached at the level of their cytoplasm every minute for 40 min to inactivate the fluorescence of chimeras returning in this compartment before measurement of residual nuclear fluorescence. Importantly, the experiment duration was chosen to avoid bias possibly due to protein degradation: EGFP/c-Fos half-life is >2.5 h and those of c-Fos/EGFP and GST/NLS/GFP are much longer (10), meaning that no detectable abundance decrease occurred during the FLIP. Loss of fluorescence was 2-fold higher in the case of EGFP/c-Fos (Fig. 1C) and c-Fos/EGFP (not shown) than for GST/NLS/GFP, which was consistent with the nucleocytoplasmic shuttling capability provided by the c-Fos moiety of the two EGFP/chimeras. Noteworthy, cytoplasmic photobleaching inactivates the fluorescence of EGFP chimera exiting the nucleus as well as that of newly synthesized proteins. It is, nevertheless, unlikely

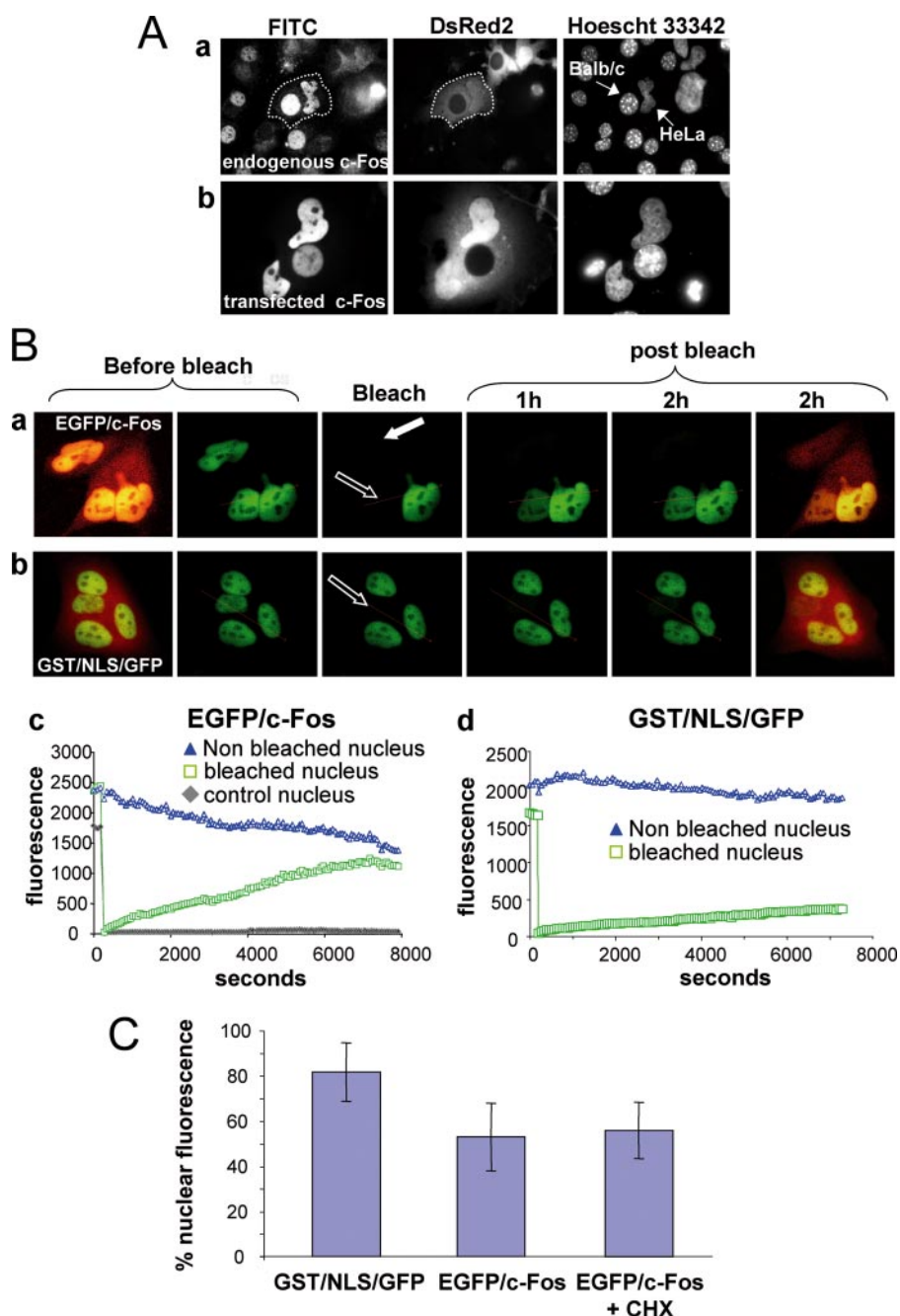


**FIGURE 1. c-Fos is a shuttling protein.** *A*, endogenous and transfected c-Fos nucleocytoplasmic shuttling in heterokaryon assays. In *a*, serum-starved BALB/c 3T3 cells were stimulated by 20% serum to allow endogenous c-Fos expression. 1 h later, HeLa cells expressing the tetrameric DsRed2 protein were added in presence of CHX for 2 h, a time sufficient to allow them to spread. The two cell types were then PEG-fused, still in the presence of CHX, fixed 1 h later, and c-Fos localization was analyzed by indirect immunofluorescence using the sc52 antibody and a fluorescein isothiocyanate-conjugated anti-rabbit antiserum. The dotted line delimits a red fluorescing heterokaryon. Notably, DsRed2 cannot enter the mouse nucleus during the course of the experiment due to its big size ( $4 \times 28$  kDa) and absence of NLS. The arrows indicate HeLa and BALB/c 3T3 nuclei with their easily distinguishable Hoescht 33342 stainings. In *b*, HeLa cells were co-transfected with plasmids for DsRed2 and c-Fos for 16 h before heterokaryon formation with asynchronously growing BALB/c 3T3 fibroblasts that do not express c-Fos. PEG fusion and microscopic analysis were carried out as in *a*. *B*, FRAP analysis of HeLa cells homopolykaryons. HeLa cells were incubated with PEG for 1 min to induce homopolykaryon formation. One hour later, cells were co-transfected with vectors expressing DsRed-monomer, a monomeric variant of DsRed that diffuses freely between the nucleus and the cytoplasm, and either EGFP/c-Fos or GST/NLS/EGFP. 19 h later, CHX was added and one nucleus (open arrow) of each homopolykaryon was laser-photobleached. Recovery of fluorescence was monitored for 2 h with one acquisition every minute. In *B*: panel *a*, the nucleus of an isolated cell was also bleached (solid arrow). Absence of fluorescence recovery showed that protein neosynthesis was efficiently inhibited by CHX. The rightmost and leftmost panels in *a* and *b* present the merged DsRed2-monomer and EGFP/c-Fos or GST/NLS/EGFP fluorescence images of the initial and final states, respectively. The FRAP curves corresponding to those in *B*, panels *a* and *b*, are presented in *B*, panels *c* and *d*, respectively. Blue and green curves correspond to fluorescence in the polykaryon bleached- and non-bleached nuclei, respectively. The gray curve corresponds to the fluorescence of the bleached nucleus of the isolated cell shown in *a*. Five independent FRAP experiments were carried out for each protein with similar outcomes. *C*, FLIP experiments on HeLa cells expressing GST/GFP/NLS and EGFP/c-Fos. HeLa cells were co-transfected to express DsRed-monomer, which helps for the positioning of the laser beam on the cytoplasm, and either GST/NLS/GFP or EGFP/c-Fos. FLIP experiments were carried out 16 h later after having, or not, stopped protein synthesis by CHX for 1 h. To this aim, cytoplasm was laser-irradiated every minute for 40 min, and the remaining nuclear fluorescence was measured after each bleach. Presented values correspond to the remaining nuclear fluorescence after 40 min of FLIP calculated from the averages of 8–10 individual cells analyzed in 3 independent transfections per experimental conditions. Error bars indicate standard deviations.

that the latter population of molecules has impinged on our data, because (i) the long life span of all chimera implicates that neosynthesized proteins constituted only a small fraction of the molecules analyzed during the experiment and (ii) addition of CHX did not interfere with the final outcomes of the experiments (Fig. 1C). Thus, c-Fos, even under condition of predominant nuclear localization, can undergo nucleocytoplasmic shuttling.

**N-terminal Domain NLS Delineation**—Various c-Fos deletion mutants and EGFP chimeras were then studied in HeLa cells to identify the regions of c-Fos involved in nuclear import. Our main results were as follows: (i) We found no evidence for an NLS located C-terminally of the DBD, *i.e.* neither within the LZ (amino acids 160–200) nor within the C-terminal domain (amino acids 200–380) (Fig. 2A), because neither LZ- (c-Fos $\Delta$ 163–196 mutant) nor C-terminal domain (c-Fos-(1–196)) deletion detectably altered c-Fos nuclear localization (Fig. 2B). Moreover, a truncated c-Fos mutant composed of only half of the DBD, the LZ, and the C-terminal domain (c-Fos-(150–380)) distributed evenly within the cell (Fig. 2B). Consistently, neither the fusion of the LZ (EGFP/c-Fos-(160–200) chimera) nor that of the C-terminal domain (EGFP/c-Fos-(200–380)) affected the naturally homogenous intracellular distribution of EGFP (Fig. 2B). (ii) We confirmed the presence of an NLS within the DBD and showed the presence of a second NLS in the N-terminal domain. Indeed, fusion of the DBD (EGFP/c-Fos-(140–159)) or of the N-terminal moiety (c-Fos-(1–139)/EGFP) to EGFP, entailed nuclear accumulation of the two chimeras (Fig. 2, C (panels g and h) and D (panels g and h)). Moreover, deletion of either the N-terminal domain (c-Fos $\Delta$ 1–139) or the DBD (c-Fos $\Delta$ 140–159) only led to partial cytoplasmic redistribution of c-Fos (30–35% and 25–30% cytoplasmic accumulation, respectively, as quantified by indirect immunofluorescence in a confocal plane) (Fig. 2, C (panels b and c) and D (panels b and c)). This indicated that quantitative nuclear accumulation of c-Fos depends on the combined action of both NLS. (iii) We mapped an element with autonomous NLS activity between amino acids 90 and 139, but we could not detect another element with comparable activity upstream of amino acid 90. Supporting this conclusion, c-Fos amino acids 90–139 (c-Fos-(90–139)/EGFP chimera) could drive EGFP in the nucleus, whereas amino acids 1–49 (not shown) or 1–90 (c-Fos-(1–90)/EGFP) could not (Fig. 2, C (panels j and i) and D (panels j and i)). Two observations also showed that full activity of this N-terminal moiety NLS depends on another upstream element in the c-Fos context. First, deletion of only the N-terminal 89 (c-Fos $\Delta$ 1–89 mutant; not shown) or 49 amino acids (c-Fos $\Delta$ 1–49 mutant) was as efficient as the removal of the whole N-terminal moiety (*i.e.* amino acids 1–139) for inducing partial (30–35%) cytoplasmic redistribution of c-Fos (Fig. 2, C (panels c and d) and D (panels c and d)). As this redistribution was comparable to that of the c-Fos $\Delta$ 1–139 mutant that still harbors the DBD NLS, this suggested complete loss of activity for the NLS located between amino acids 90 and 139 in c-Fos $\Delta$ 1–49 and c-Fos $\Delta$ 1–89. Second, the deletion of both amino acids 1–49 and the DBD (c-Fos $\Delta$ 1–49 $\Delta$ 140–159 mutant) led to an even distribution of c-Fos throughout of the cells. This was indicative of total loss of

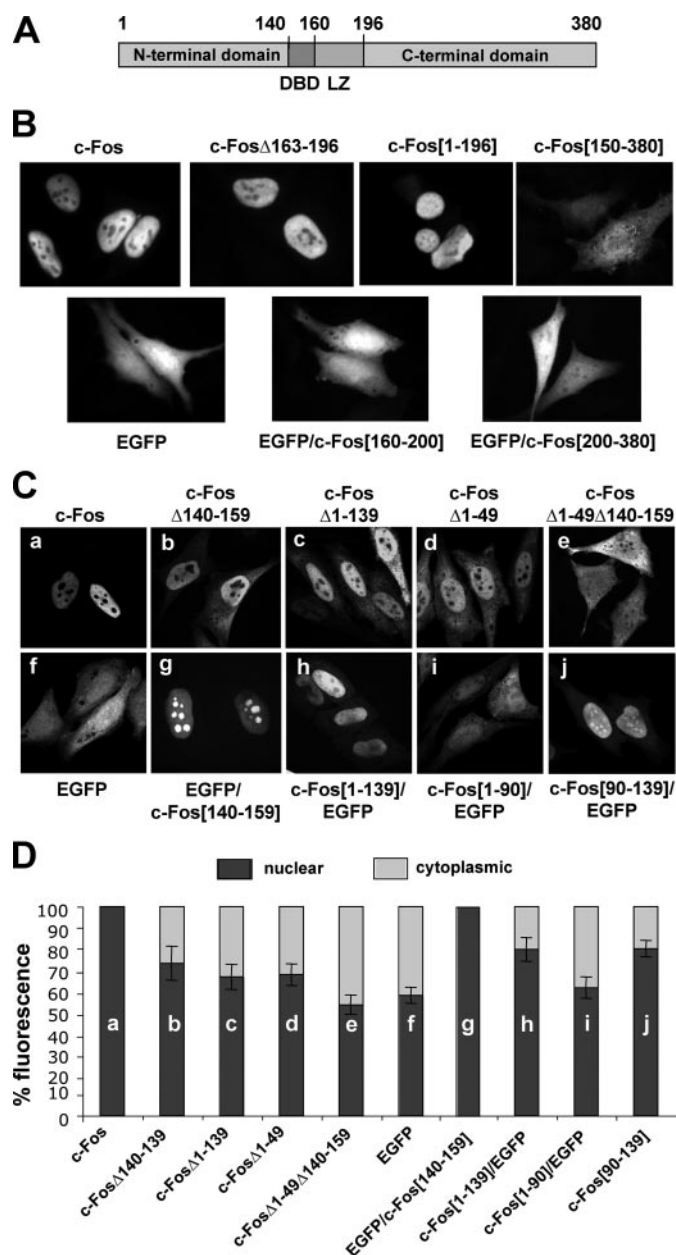


**FIGURE 2. Identification of the second c-Fos NLS.** A, schematic structure of c-Fos. DNA-binding domain (DBD) and leucine zipper (LZ) are indicated. Numbers correspond to amino acid positions. B, absence of NLS in the LZ and the C-terminal domain of c-Fos. HeLa cells were transfected with expression vectors encoding the indicated c-Fos mutants and EGFP/c-Fos chimeras. 16 h later, the intracellular localization of the mutants was determined by indirect immunofluorescence using the anti-c-Fos H125 rabbit antiserum and Alexa488-conjugated anti-rabbit antiserum. Chimeras were detected by direct fluorescence. C, NLS activity is carried by the N-terminal domain of c-Fos. The experiments were conducted as in B, except that observations were performed using a confocal microscope. Each construct was analyzed in three to six independent transfection experiments. D, nuclear versus cytoplasmic distribution of the constructs presented in C. Nuclear and cytoplasmic fluorescences were quantified using the Metamorph software in 30 cells for each construct. The histograms correspond to fluorescence percentages in the nucleus and in the cytoplasm with respect to total cell fluorescence in the section analyzed. Error bars indicate standard deviations.

NLS activity by the domain of amino acids 90–139 that was left intact in c-Fos $\Delta$ 1–49 $\Delta$ 140–159 (Fig. 2, C (panel e) and D (panel e)). Moreover, the latter data also indicated the absence of a third NLS in c-Fos.

## c-Fos Nucleocytoplasmic Traffic

*Transportin 1 Contributes to N-terminal NLS-mediated c-Fos Nuclear Import in Vivo*—*In vitro*, Imp $\beta$ 1 and TRN1 can mediate DBD- and N-terminal NLS-dependent c-Fos nuclear transport, respectively (23). We therefore addressed whether this was also the case *in vivo*. Cytoplasmic *versus* nuclear accumulation of both c-Fos deletion mutants and EGFP chimeras harboring only one of the two NLS were consequently quantified in HeLa cells subjected to RNA interference against different importins. Not only were Imp $\beta$ 1 and TRN1 considered, but also TRN2, because this latter import receptor displays high similarity and partial functional redundancy with TRN1 (40, 41). As a control, we used Imp7 depletion, which, at least *in vitro*, has been shown not to participate in c-Fos nuclear import (23).

c-Fos-(1–139)/EGFP/GST is a chimeric protein made up of the N-terminal moiety of c-Fos, EGFP, and GST. Due to its molecular mass (80 kDa) and ability to dimerize owing to its GST part, it cannot diffuse passively through the nuclear pore, which permits accurate monitoring of c-Fos N-terminal NLS activity. Under control conditions, 44% of cells expressed <30% of c-Fos-(1–139)/EGFP/GST in the cytoplasm and 55% of them between 30 to 50% (Fig. 3, A and B). No significant change in c-Fos distribution was observed in the presence of siRNAs against TRN2, Imp $\beta$ 1, or Imp7 (Fig. 3B) despite an effective reduction (60–70% for TRN2 and 90% for Imp $\beta$ 1 and Imp7) in nuclear import receptor abundance (Fig. 3C). By contrast, transfection of anti-TRN1 siRNAs shifted the accumulation of c-Fos-(1–139)/EGFP/GST toward a predominant cytoplasmic localization in 40% of the cells with >50% of the protein within the cytoplasm (Fig. 3B). Interestingly, RNA interference against both TRN1 and TRN2 increased neither the percentage of c-Fos-(1–139)/EGFP/GST within the cytoplasm nor the fraction of cells with >50% of the protein within the cytoplasm (Fig. 3B). This suggested that TRN1 and TRN2 do not cooperate for N-terminal NLS-mediated nuclear transport of c-Fos. This was an important verification, because the anti-TRN1 siRNA alone led to a reproducible increase in TRN2 level (Fig. 3C) that might have compensated for the reduction in TRN1 activity. Strengthening the idea of TRN1 involvement in N-terminal NLS-dependent c-Fos nuclear transport, similar data were obtained when the cytoplasmic *versus* nuclear distributions of the DBD-lacking c-Fos $\Delta$ 140–159 mutant and the EGFP/c-Fos $\Delta$ 140–159 chimera were investigated (not shown).

Next, because Imp $\beta$ 1 was shown to interact with c-Fos DBD *in vitro* (23), we investigated whether Imp $\beta$ 1 is involved in basic NLS-mediated c-Fos nuclear import *in vivo* using two chimeras: EGFP/c-Fos-(140–200), involving the b-Zip domain, and EGFP/c-Fos-(140–380), containing the bZip plus the c-Fos C-terminal domain. No increase in cytoplasmic localization was observed in any of our multiple siRNA transfection experiments. Absence of effect must, however, be interpreted cautiously. Although the amount of the importin was reduced by 90%, it cannot be excluded that its residual level was still sufficient for nuclear transport of c-Fos-EGFP chimeras. This possibility was to be considered, because attempts to obtain stronger repression by repeated transfections and/or use of increasing amounts of anti-Imp $\beta$ 1 siRNA repeatedly led to dramatic cell death, whereas apoptosis was limited under the con-

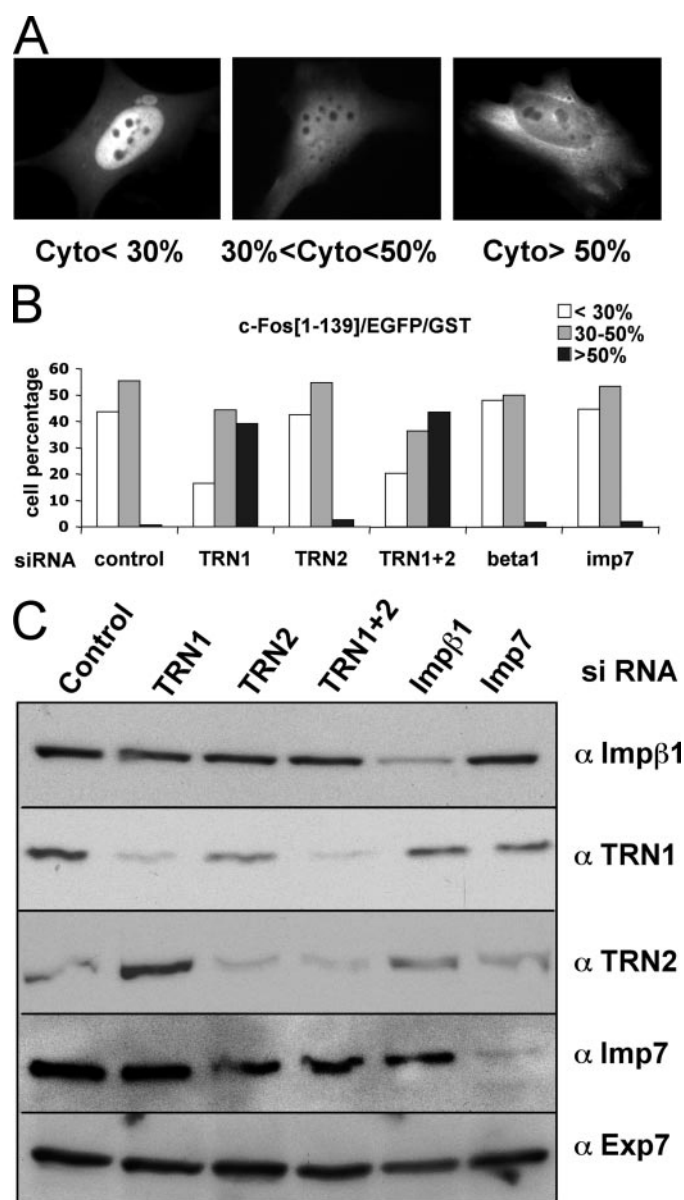


**FIGURE 3. TRN1 contributes to c-Fos nuclear import via the N-terminal NLS.** A, cell classification according to the cytoplasmic *versus* nuclear localization of c-Fos-(1–139)/EGFP/GST. HeLa cells were transfected to express c-Fos-(1–139)/EGFP/GST. 16 h later, fluorescence was analyzed by confocal microscopy and the percentages of cytoplasmic and nuclear c-Fos-(1–139)/EGFP/GST were quantified using the Metamorph software. Cells were classified in three groups according to the fraction of c-Fos found in the cytoplasm, *i.e.* <30%, between 30 and 50%, and >50%. Figures representative of each group are presented. B, effect of anti-importin siRNAs on the localization of c-Fos-(1–139)/EGFP/GST. HeLa cells were transfected with the various siRNA and, 36 h later, with the c-Fos-(1–139)/EGFP/GST. 16 h later, at least 100 cells were analyzed for classification as described in A. Three independent experiments were conducted with similar outcomes. C, immunoblotting characterization of siRNA effects. Extracts from cells transfected as in B were analyzed by immunoblotting with the indicated anti-importin antisera. Exportin 7 was used as an invariant control.

ditions used in experiments such as that presented in Fig. 3. Similar to Imp $\beta$ 1, no effect was observed for Imp7 and TRN2 knockdowns (see “Discussion”). Thus, whereas we cannot conclude on the role of Imp $\beta$ 1, we show a clear role for TRN1 in N-terminal NLS-mediated nuclear import of c-Fos *in vivo*.

*c-Fos Exits the Nucleus Independently of Crm1*—Because (i) various shuttling transcription factors are exported from the

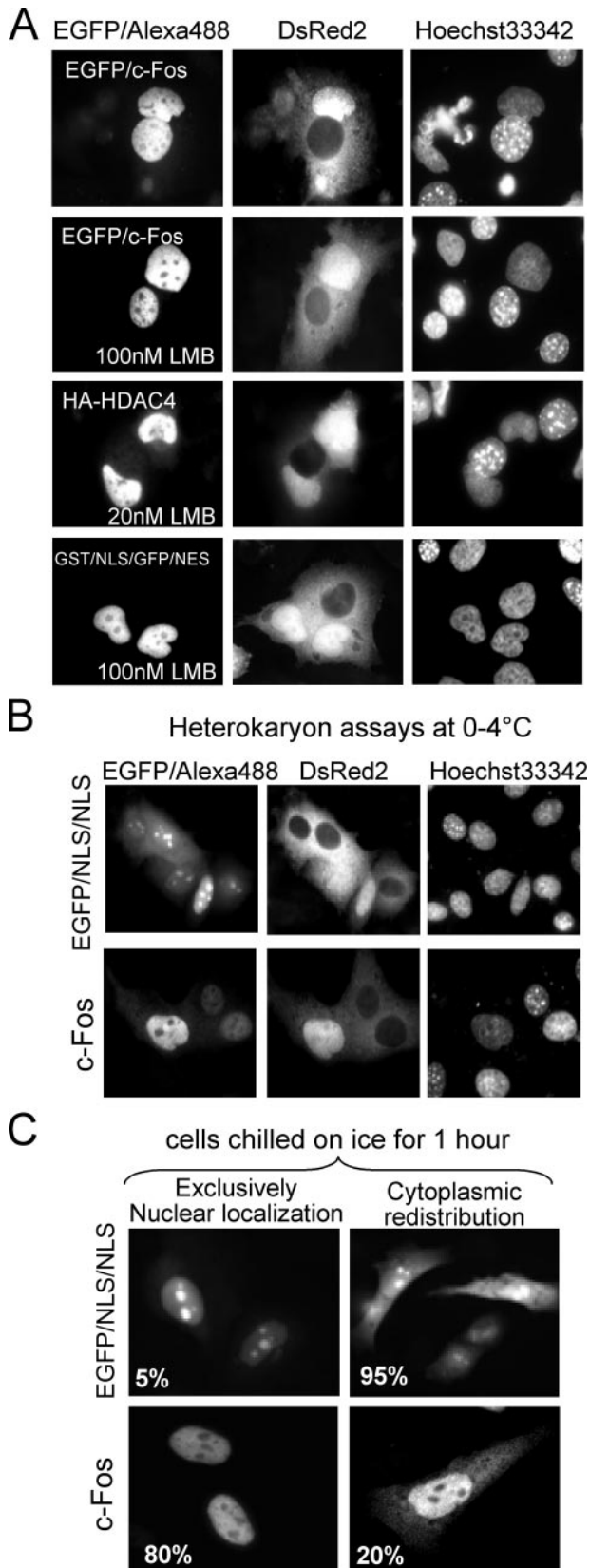


**FIGURE 4. c-Fos shuttling is an active process and is not inhibited by leptomycin.** *A*, heterokaryon experiments in presence of LMB. BALB/c 3T3 fibroblasts were PEG-fused to HeLa cells co-expressing DsRed2 protein and either EGFP-c-Fos, HA-tagged HDAC4, or GST/NLS/GFP/NES after 1 h pretreatment of both cell types with CHX and the indicated concentrations of LMB. Heterokaryons were incubated at 37 °C for 1 h in the presence of the two

nucleus by the LMB-sensitive Crm-1 exportin (42), (ii) c-Fos contains three motifs showing similarities with NES recognized by Crm1 (43), and (iii) c-Fos cytoplasmic accumulation in cells with activated STAT3 and inactive Erk5 is inhibited by LMB (14), we tested Crm-1 implication in c-Fos nuclear export in heterokaryon experiments. Our results showed that addition of LMB, up to a concentration of 100 nM, could not inhibit c-Fos shuttling, whereas under the same experimental conditions the shuttling of HDAC4 (44) and that of the chimeric protein GST/NLS/GFP/NES, a GST/GFP chimera containing both the SV40 LT antigen NLS and the LMB-sensitive HIV Rev NES (43), were fully blocked (Fig. 4). Thus, in cells predominantly accumulating c-Fos in the nucleus, c-Fos nuclear export does not depend on the classic LMB-sensitive CRM1 pathway.

It was then important to ask whether c-Fos is exported into the cytoplasm passively or via an active mechanism. To this aim, we first conducted heterokaryon assays under conditions where active nuclear import and export are inhibited by shift to low temperature, whereas passive diffusion through the nucleopore complex is not (45, 46). In these experiments, c-Fos shuttling was compared with that of EGFP/NLS/NLS, because the latter protein (i) is efficiently imported into the nucleus, due to the presence of a duplicated SV40 LT antigen NLS, (ii) it is not actively exported back to the cytoplasm, due to the absence of an NES, (iii) it can diffuse passively between the nucleus and the cytoplasm because of its relatively small size, and (iv) its size is comparable to that of c-Fos. Transfected HeLa cells expressing either c-Fos or EGFP/NLS/NLS were PEG-fused to BALB/c 3T3 cells, left at 37 °C for 15 min to allow completion of heterokaryon formation, and then either incubated on ice or at 37 °C (controls) for another 45 min before cell fixation and microscope analysis. At the end of the experiment at 37 °C, EGFP/NLS/NLS was exclusively found in donor and acceptor nuclei with no cytoplasmic signal as active nuclear import largely dominates over passive leakage of the protein out of the nucleus (not shown). In contrast, at 0 °C, EGFP/NLS/NLS was found distributed between the nuclei and the cytoplasm in the majority of heterokaryons because its propensity to diffuse throughout the cell could no longer be compensated by reimport into the nucleus (Fig. 4*B*). In the case of c-Fos, shuttling activity (Fig. 1) was confirmed at 37 °C with equal labeling of donor and acceptor nuclei (not shown). In contrast, at 0 °C, the protein was essentially found within the donor nuclei of nearly all heterokaryons with only low fluorescence signals in the acceptor ones (Fig. 4*B*). This indicated that, at low temperature, passive

drugs and then fixed. HDAC4 was detected by indirect immunofluorescence with the 3F10 anti-HA rat monoclonal antibody and Alexa488-conjugated anti-rat antiserum. EGFP chimeras were detected by direct fluorescence. *B*, c-Fos shuttling efficiency assayed in heterokaryons at low temperature. HeLa cells expressing DsRed2 and either EGFP/NLS/NLS or c-Fos were PEG-fused to BALB/c 3T3 cells. 15 min after fusion, they were either maintained at 37 °C (control condition; not shown; see text) or placed on ice for 45 min to inhibit active nuclear import and export. c-Fos was detected using the sc-52 goat antibody and an Alexa488-labeled anti-goat antiserum. Typical results are presented for both c-Fos and EGFP/NLS/NLS. *C*, c-Fos distribution at low temperature. HeLa cells transfected with plasmids encoding either EGFP/NLS/NLS or c-Fos were incubated on ice for 1 h before fixing and microscope analysis. c-Fos was detected as in *B*. The percentage of cells with a strictly nuclear localization or with a cytoplasmic redistribution is indicated. >300 cells were counted for each transgene.

## c-Fos Nucleocytoplasmic Traffic

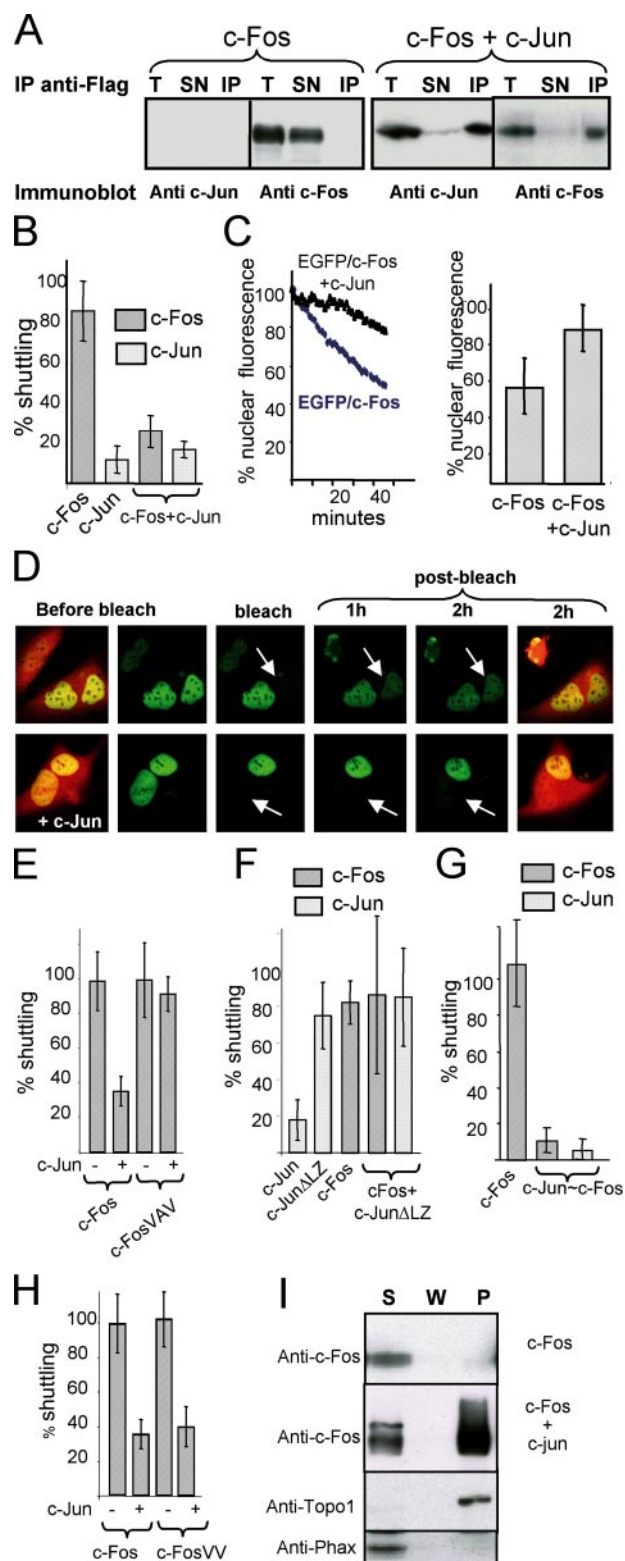


**FIGURE 5. Dimerization with c-Jun inhibits c-Fos shuttling.** *A*, c-Fos heterodimerizes with c-Jun upon co-transfection. HeLa cells were co-transfected with equivalent amounts of plasmids encoding c-Fos and/or c-Jun C-terminally-tagged with the FLAG epitope. 16 h post-transfection, immunoprecipitation was carried out using the anti-FLAG M2 monoclonal antibody coupled to agarose beads. Immunoblots of the three fractions (*T*, total cell extract; *SN*, supernatant; and *IP*, immunoprecipitate) corresponding to the same initial volume of extract were probed with the sc52 anti-c-Fos or sc45 anti-c-Jun rabbit antisera. *B*, heterokaryon assays. HeLa cells were co-transfected with plasmids for DsRed2 and c-Fos, c-Jun, or c-Fos plus c-Jun. 16 h later they were

diffusion of c-Fos out of the nucleus is poorly efficient. In fact, it is very likely that the low labeling of acceptor nuclei largely resulted from active retrotransport during the 15 min required for completion of heterokaryon formation after PEG treatment. Strengthening our conclusion, EGFP/NLS/NLS largely redistributed toward the cytoplasm in most transfected cells (95%) upon simple chilling of cells owing to its diffusion ability, whereas c-Fos localization was hardly affected as it remained exclusively nuclear in 80% of transfected cells and predominantly nuclear in the other 20% (Fig. 4C).

**Heterodimerization with c-Jun Negatively Regulates c-Fos Shuttling**—Because active AP-1 complexes are dimeric, we then asked whether heterodimerization with c-Jun could impact on c-Fos nuclear export. To this aim, we monitored nucleocytoplasmic shuttling under conditions of forced or impaired dimerization.

First, we assessed whether c-Jun itself could shuttle, when transfected alone, and affect c-Fos shuttling in co-transfection experiments. This was tested in heterokaryon assays. Importantly, the two proteins were expressed using identical amounts of similar cytomegalovirus promoter-based vectors. Because c-Jun is slightly more stable than c-Fos and as c-Fos:c-Jun heterodimer formation is favored over that of c-Jun:c-Jun homodimers (6), this ensured a significant excess of c-Jun over c-Fos and quantitative engagement of the latter protein in c-Jun:c-Fos dimers as shown in co-immunoprecipitation experiments (Fig. 5A). Heterokaryon assays showed that c-Jun

PEG-fused with BALB/c 3T3 fibroblasts. c-Fos and c-Jun protein shuttling was assayed 1 h post fusion. c-Fos was detected using the sc52 goat antibody and an Alexa488-labeled anti-goat antiserum, whereas c-Jun was detected with the sc45 rabbit antibody and an Alexa647-labeled anti-rabbit antiserum. The emission spectra of the two dyes are sufficiently different to avoid any signal cross-contamination. The shuttling efficiency is calculated as the ratio of the fluorescence in the acceptor nucleus versus that in the donor one. *Hatched histograms* correspond to quantification of c-Fos Alexa488 signals, whereas *dotted ones* correspond to quantification of c-Jun Alexa647 signals. The presented values are the average of values obtained from at least 20 heterokaryons per experimental condition. The *bars* correspond to standard deviations. Three independent experiments were conducted with similar outcomes. *C*, FLIP analysis. The shuttling of EGFP/c-Fos in presence of c-Jun was monitored by FLIP under the same conditions as in Fig. 1D. Ten FLIP experiments were carried out. Typical curves of nuclear fluorescence decrease as a function of time are presented in the *left panel*. The *histograms* in the *right panel* give the values of the remaining nuclear fluorescence after 40 min of FLIP. *Error bars* correspond to standard deviations. The presented data were obtained in the absence of CHX. Similar results were obtained in its presence. *D*, FRAP analysis. FRAP experiments in c-Fos-expressing HeLa cells were carried out as described in Fig. 1B in the absence (*upper panels*) or in the presence (*lower panels*) of c-Jun. An *arrow* indicates the bleached nucleus in each HeLa homopolykaryon. *E–H*, shuttling efficiencies of c-Fos and c-Jun mutants. Shuttling efficiencies were assayed in heterokaryon assays as in *B*. *Hatched histograms* correspond to c-Fos shuttling analysis, and *dotted ones* correspond to c-Jun shuttling analysis. *E*, corresponds to comparison of wild-type c-Fos with the non-dimerizable c-FosVAV mutant in the presence and in the absence of c-Jun. *F*, corresponds to the comparison of wild-type c-Jun with the non-dimerizable c-JunΔLZ mutant in the presence and in the absence of c-Fos. *G*, corresponds to the comparison of c-Fos with the tethered c-Jun~c-Fos dimer. Analysis of the localization of the latter was performed with both anti-c-Fos and anti-c-Jun antibodies. *H*, corresponds to the comparison of wild-type c-Fos with the non DNA-binding c-FosVV mutant in the presence and in the absence of c-Jun. *I*, heterodimeric c-Fos is associated with a non-soluble nuclear fraction. Fractionation experiments were carried out as described under “Experimental Procedures” in the presence of Triton X-100 using asynchronous transiently transfected HeLa cells expressing c-Fos either in absence or in presence of c-Jun. Topoisomerase 1 and Phax were used as markers of the non-soluble and soluble fractions, respectively (*S* = cytoplasmic and soluble nuclear proteins, *W* = wash fraction containing protein loosely attached to chromatin and nuclear matrix, *P* = insoluble proteins of the chromatin- and the nuclear matrix).

transfected alone shuttles very poorly compared with c-Fos when transfected alone (Fig. 5B). Moreover, its expression reduced the shuttling of c-Fos by 3-fold, whereas c-Fos did not affect c-Jun shuttling in co-transfection experiments (Fig. 5B). Two observations strengthened the notion of c-Fos shuttling inhibition by c-Jun. First, cytoplasmic photobleaching in FLIP experiments showed that ectopic c-Jun slowed down EGFP/c-Fos return to the cytoplasm (Fig. 5C). Second, 24 h after PEG-induced formation of HeLa cell homopolykaryons, nuclear fluorescence of EGFP/c-Fos was not recovered in the presence of c-Jun 2 h after nuclear FRAP while almost complete recovery was seen in its absence (Fig. 5D).

We then addressed whether inhibition of c-Fos shuttling was due to physical association with c-Jun or to possible indirect effects of the latter protein. To this aim, we analyzed the behavior of a dimerization-deficient mutant of c-Fos (47) in heterokaryon experiments. This mutant (c-FosVAV) shuttled similarly to wild-type c-Fos transfected alone, but its shuttling activity was not slowed down by the presence of co-transfected wild type c-Jun (Fig. 5E). Moreover, wild-type c-Fos shuttling was not inhibited by the presence of a dimerization-deficient LZ-less c-Jun mutant (c-Jun $\Delta$ LZ) (Fig. 5F). Taken together, these data indicate that inhibition of c-Fos shuttling is primarily due to physical association with c-Jun. Interestingly, in contrast to wild-type c-Jun, the non-dimerizable c-Jun $\Delta$ LZ mutant shuttled efficiently in heterokaryon assays (Fig. 5F). This suggests that homodimerization also prevents efficient c-Jun shuttling.

Because c-Fos and c-Jun undergo dynamic and rapid association and dissociation cycles *in vivo* (38), we then tested whether stabilizing dimerization could further limit nucleocytoplasmic shuttling. This was done using a "tethered dimer" (c-Jun~c-Fos) displaying the essential functional and biological properties of the natural c-Jun:c-Fos dimer in various settings (32). In this chimera, the c-Fos and c-Jun moieties are brought together within the same molecule by a flexible peptide linker. Because intramolecular interactions are favored over intermolecular ones with other LZ-harboring proteins, this ensures both specific and stronger interactions between c-Fos and c-Jun. In heterokaryon assays, the shuttling efficiency of this chimera was 10- to 15-fold less than that of c-Fos alone and 3- to 6-fold less than that of c-Fos in the presence of ectopic c-Jun (Fig. 5G). Taken with the afore-mentioned data, this indicated that LZ-mediated dimerization is crucial for inhibition of, not only the shuttling of c-Fos, but also that of c-Jun.

Finally, because dimerization of c-Fos and c-Jun may be followed by recognition of genomic AP-1 motifs in transfected cells, we assessed whether inhibition of shuttling was primarily due to dimerization or to binding to DNA. It is of note that the latter may possibly be followed by target gene transcription activation and, thereby, indirect retrocontrol of the protein localization. Because a c-Fos DNA binding-defective mutant (c-FosVV) (48) behaves as c-Fos in heterokaryon assays performed both in the presence and in the absence of c-Jun (Fig. 5H), the primary reason for inhibition of c-Fos shuttling is dimerization with c-Jun and not recognition of target DNA sequences or indirect effect resulting from target gene activation.

Then, we asked whether inhibition of c-Fos export upon heterodimerization with c-Jun was simply due to NES masking or to association with nuclear components/structures. To achieve this, c-Fos intranuclear distribution in the presence or in the absence of c-Jun was addressed in cell fractionation experiments of transfected HeLa cells in the presence of the mild detergent Triton X-100 as described elsewhere (16). This allowed to isolate (i) a fraction containing the cytoplasmic and soluble nuclear proteins (S) and (ii) an insoluble fraction containing both the chromatin and the nuclear matrix (P) and a "wash fraction" (W) containing the proteins loosely attached to the insoluble components of the nucleus. The data presented in Fig. 5I show that c-Fos is predominantly soluble in the absence of c-Jun and predominantly insoluble in its presence. Thus, retention of c-Fos within the nucleus is unlikely to result from simple NES masking by c-Jun but rather from association with nuclear structure/components it cannot associate with alone.

The above experiments were conducted in transient transfection assays of exponentially growing cells. We next wished to investigate the effect of dimerization on c-Fos shuttling activity in a more physiological situation. To achieve this, we turned again to re-entry of quiescent cells into the cell cycle, because c-Fos dimerizes with the various endogenous Jun proteins expressed under these conditions (49). To avoid interference with endogenous c-Fos, the experiments were conducted in f10 cells, which are mouse embryo fibroblasts derived from mice KO for *c-fos* gene (34). These cells were stably transfected with vectors (i) expressing either EGFP-c-Fos or its non-dimerizable variant EGFP-c-Fos $\Delta$ LZ and (ii) recapitulating the transient expression of the normal *c-fos* gene upon stimulation by serum owing to a minimal serum-responsive element-containing *c-fos* promoter and the *c-fos* 3'-untranslated region containing the major mRNA destabilizer (Fig. 6A; see Refs. 9, 10, 12, 13 for more details). Importantly, similar levels of the two chimeras were induced in the selected transfectant populations as assayed by immunoblotting (not shown), which ruled out possible biases linked to differences in protein abundance. The shuttling efficiencies of the two EGFP-c-Fos chimera were then compared in heterokaryon assays made between serum-stimulated f10 transfectant and asynchronous HeLa cells. The data presented in Fig. 6 (B and C) show that EGFP-c-Fos $\Delta$ LZ shuttles twice more efficiently than EGFP-c-Fos during the G<sub>0</sub>/G<sub>1</sub> transition, as estimated from lower fluorescence intensity in acceptor nuclei for the latter protein. This supports the idea that heterodimerization also exerts a negative effect on c-Fos shuttling under physiological conditions of expression.

*JunB and JunD Are Less Efficient at Inhibiting c-Fos Shuttling than c-Jun*—Heterokaryon assays, then, showed that both JunB and JunD are more efficient at nucleocytoplasmic shuttling than wild-type c-Jun when transfected alone (Fig. 7A). They were also less efficient at inhibiting c-Fos return into the cytoplasm (Fig. 7B). This was not due to intrinsic inability to dimerize with c-Fos as co-immunoprecipitations showed quantitative association between c-Fos and the two Jun proteins (Fig. 7C). Co-immunoprecipitations, however, give steady-state indications but none on dedimerization/redimerization kinetics. Because affinities of JunB and JunD for c-Fos are lower than that

## c-Fos Nucleocytoplasmic Traffic

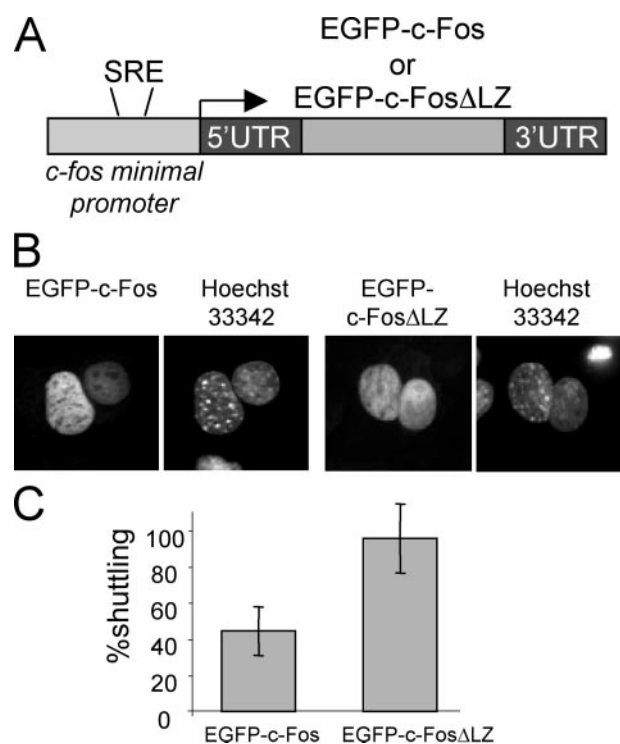


**FIGURE 6. Heterodimerization inhibits c-Fos shuttling during the  $G_0/G_1$  transition.** *A*, expression vectors recapitulating the transient serum-induced expression of *c-fos* gene. cDNA for EGFP-c-Fos or EGFP-c-Fos $\Delta$ LZ were cloned in a vector recapitulating the transient expression of the *c-fos* gene in normal cells during the  $G_0/G_1$  phase transition upon stimulation by serum owing to both a minimal *c-fos* gene promoter containing the serum-responsive element and the *c-fos* mRNA 3' untranslated region. *B*, typical heterokaryon assays using mouse cells traversing the  $G_0/G_1$  phase transition. Serum-starved *c-fos*<sup>-/-</sup> f10 cells stably transfected with the plasmids described in *A* were stimulated by serum for 1 h. They were then PEG-fused to asynchronous HeLa cells and fixed 1 h later for microscopic observation. *C*, shuttling efficiencies of EGFP-c-Fos and EGFP-c-Fos $\Delta$ LZ. Fluorescence in the donor and acceptor nuclei was measured as described in Fig. 5*B* for >50 heterokaryons in each case.

of c-Jun (6, 50), dedimerization occurs more frequently in the case of the former two proteins, which may increase c-Fos availability for nuclear export. We therefore tested whether forcing dimerization with JunB could inhibit c-Fos nuclear export. Appropriate tethered dimers with fully characterized phenotype not being available, we used a bimolecular fluorescence complementation (BiFC) assay (Hu *et al.* 28), in which the N-terminal moiety of the fluorescent YFP protein was N-terminally fused to c-Fos (YFP-(1–154)/c-Fos), whereas its C-terminal moiety was N-terminally fused to JunB (YFP-(155–238)/JunB). Neither YFP-(1–154)/c-Fos nor YFP-(155–238)/JunB fluoresces by itself, and the two halves of YFP cannot reassociate on their own. By contrast, LZ-mediated heterodimerization of c-Fos and JunB triggers YFP reformation, which is followed by both fluorescence reemission and stabilization of the dimer (28). In heterokaryon assays, fluorescent heterodimers formed by YFP-(1–154)/c-Fos and YFP-(155–238)/JunB shuttled inefficiently with hardly detectable signals in acceptor cells (Fig. 7*D*, panel *a*). Similar results were obtained, in parallel, with YFP-(1–154)/c-Fos and a YFP-(155–238)-c-Jun chimera (Fig. 7*D*, panel *b*).

Thus, JunB and JunD are shuttling proteins capable of inhibiting c-Fos nuclear export, albeit less efficiently than c-Jun.

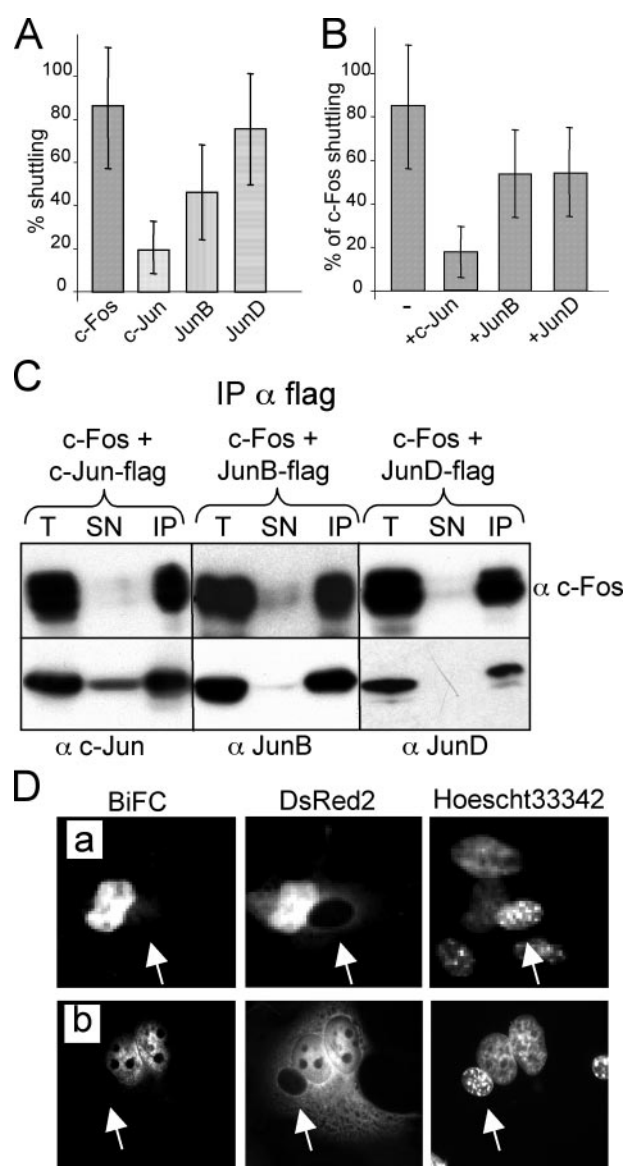


**FIGURE 7. Differential inhibition of c-Fos shuttling by Jun family members.** *A*, relative shuttling efficiencies of c-Fos, c-Jun, JunB, and JunD transfected alone in heterokaryon assays. Experiments were carried out as in Fig. 5*B* using HeLa cells as donors and BALB/c 3T3 cells as acceptors, and quantifications were carried out as in Fig. 5*B*, c-Fos, c-Jun, JunB, and JunD were detected using the goat sc52G, rabbit sc45, the goat sc46G, and rabbit sc74 antibodies, respectively, and anti-goat or anti-rabbit Alexa488-conjugated secondary antibodies. *B*, inhibition of c-Fos shuttling by Jun proteins in standard heterokaryon assays. Experiments were conducted as in Fig. 5*B*. c-Fos was detected using the sc52 goat antibody and an Alexa488-labeled anti-goat secondary antibody. c-Jun, JunB, and JunD were detected with the sc-45, sc-46G, and sc-74 antibodies, respectively, and Alexa 647-labeled anti-rabbit antibodies. *C*, heterodimerization of c-Fos with Jun family members. HeLa cells were co-transfected with equivalent amounts of plasmids encoding c-Fos and either c-Jun, JunB, or JunD. All JunB were C-terminally tagged with the FLAG epitope. Immunoprecipitations and immunoblots were performed as described in Fig. 5*A*. *D*, inhibition of c-Fos shuttling by JunB or c-Jun in BiFC assay. HeLa cells were transfected to express DsRed2 in the presence of either YFP-(1–154)/c-Fos and YFP-(155–238)/JunB (upper panels) or YFP-(1–154)/c-Fos and YFP-(155–238)/c-Jun (lower panel) and PEG-fused to BALB/c fibroblasts 24 h later. Localization of YFP fluorescence-emitting dimers was assayed 1 h later after fixation and Hoechst 33342 nucleus staining.

## DISCUSSION

The present study refines our understanding of c-Fos transport into the nucleus and shows that c-Fos, as well as other

AP-1 family proteins, undergoes regulated nucleocytoplasmic shuttling even under conditions of predominant nuclear localization.

**Nuclear Import of c-Fos**—Here, we have localized the second c-Fos NLS within the N-terminal domain and shown that the combined action of the two NLSs is required for quantitative c-Fos nuclear accumulation. Several lines of evidence suggest a complex and conformation-dependent activity for the N-terminal NLS. First, amino acid sequence examination excludes the presence of a classic short, lysine- or arginine-rich NLS in c-Fos N-terminal moiety. Second, EGFP chimera analyses indicate an NLS with autonomous activity between amino acids 90 and 139, but none between amino acids 1 and 89. This observation is consistent with the fact that amino acids 111–124 are necessary for *in vitro* binding of TRN1 to c-Fos (23). Third, loss of activity of the 90–139 region NLS is observed upon deletion of c-Fos N-terminal 49 amino acids as shown by the even nucleocytoplasmic distribution of c-Fos $\Delta$ 1–49 $\Delta$ 140–159. The simplest explanation for this is that elements located within the N-terminal amino acids contribute to the structuration of c-Fos N-terminal moiety and, thereby, accessibility of the 90–139 NLS-carrying region. Precise molecular characterization of this NLS may require solving the crystal structure of a complex made up of c-Fos-(1–139) and the cognate karyopherin in addition to further genetic experiments such as those presented here.

Partial cytoplasmic accumulation of a c-Fos mutant deleted of amino acids 160–380 in a fraction of transfected Cos-1 cells has led others to propose an NLS activity in c-Fos C-terminal moiety (19), which neither us nor Tratner and Verma (18) could confirm. Cell-type specific effects may explain this discrepancy. Whatever the case, the activity of this third NLS, if any, is poor (19) as compared with those contained in the DBD and the N-terminal domain (18).

Others proposed that heterodimerization is a prerequisite for efficient c-Fos nuclear import. This conclusion was based on cell microinjection experiments showing that c-Fos cannot enter the nucleus unless c-Jun is co-expressed (51). This is in apparent contradiction with the following observations. First, when a c-fos vector is transfected in the absence of any Jun expression plasmid, numerous laboratories have described nuclear accumulation of c-Fos, whatever the cell context used. Second, an LZ-less c-Fos accumulates quantitatively within the nucleus (18). Third, EGFP (this work) or chicken pyruvate kinase (18) chimeras harboring one, or the two, c-Fos NLS, but not the LZ, also efficiently enter the nucleus. Fourth, in co-transfection experiments, a NLS-less c-Jun principally localizes within the cytoplasm, whereas c-Fos essentially accumulates in the nucleus (data not shown) even though the two proteins have kept their ability to dimerize via their LZ. One possibility to reconcile all of these observations is to consider the differences in experimental conditions. In all experiments where c-Fos accumulates in the nucleus independently of dimerization with c-Jun, cells were cultured in the presence of mitogens, whereas the microinjections were carried out in the presence of staurosporine, which inhibits various kinases. Because c-Fos nuclear transport is dependent on extracellular signals relayed by various intracellular signaling cascades (see the introduction), it is

possible that nuclear transport of c-Fos is inhibited by this drug and that dimerization with c-Jun permits to overcome this inhibition.

Our attempts to define the *in vivo* contributions of different nuclear import receptors for c-Fos clearly demonstrate that TRN1 has a major function for the NLS located in the N-terminal region. This result is consistent with the *in vitro* data of Arnold *et al.* (23). The contribution of the other importins to c-Fos nuclear import *in vivo* remains unclear. In the limit of their sensitivity, our siRNA experiments do not favor an implication of TRN2 meaning that c-Fos nuclear transport would depart from that of other proteins, such as HnRNPA1 and HuR (40, 41), for which TRN1 and TRN2 are redundant, at least in *in vitro* assays. For knockdown of Imp $\beta$ 1, we did not observe any effect on c-Fos nuclear import mediated by the basic NLS residing in the DBD. However, complete depletion of Imp $\beta$ 1 is lethal to cells. Therefore, the remaining low levels of residual Imp $\beta$ 1 might have been sufficient for nuclear import of c-Fos under our experimental conditions. Moreover, it has recently been demonstrated that some cargoes access multiple import pathways using the same NLS to interact with different transport receptors (52), indicating redundancy and, thereby, limits of *in vivo* siRNA approaches.

**Nuclear Export of c-Fos**—Our work adds another layer of complexity to the regulation of c-fos gene as it indicates that c-Fos protein undergoes nucleocytoplasmic shuttling, even under condition of predominant nuclear localization, and has sufficient time in its lifespan to undergo several rounds of nuclear import and export. Moreover, taken with Sasaki *et al.*'s observation (14), that c-Fos induced by STAT3 in the presence of inactivated Erk5 accumulates in the cytoplasm due (at least in part) to active nuclear export, it indicates that there exist several mechanisms for cytoplasmic return of c-Fos for at least two reasons. First, contrasting with LMB-sensitive retrotransport of c-Fos in Sasaki *et al.*'s experiments, c-Fos nuclear export was independent of Crm-1 under our experimental conditions. Importantly, return into the cytoplasm in the latter case depends on active transport rather than on passive diffusion as shown by both the absence of cytoplasmic redistribution of c-Fos in chilled cells and lack of shuttling activity in heterokaryon experiments conducted at low temperature. Second, none of the many other c-Fos mutants and EGFP chimeras we have analyzed (this work and data not shown) showed preferential or exclusive cytoplasmic accumulation. This prevented any precise NES characterization, including at the level of the domain of amino acids 223–232 whose integrity is required for cytoplasmic return in Sasaki *et al.*'s experiments. Nevertheless, the possibility of an NES in the 90–139 region has to be considered. On one hand, c-Fos-(90–139)/EGFP (as well as c-Fos-(1–139)/EGFP) partially accumulates within the cytoplasm, and, on the other hand, this region is crucial for interaction with TRN1, many substrates of which are shuttling proteins with overlapping signals for nuclear import and export (53, 54). Moreover, Crm1-independent export signals have recently been described (55).

Another important point of our study is inhibition of c-Fos nuclear export by the Jun proteins as we show that dimerization is crucial, not only for the formation of active AP-1 transcrip-

tion complexes, but also for keeping them in the nucleus where they play their transcriptional parts. At this stage of our investigations, the biological reason of c-Fos return into the cytoplasm remains unclear. A first possibility is that monomeric c-Fos may be more efficiently degraded in the cytoplasm than in the nucleus. This would be in line with the observations that (i) cytoplasmic c-Fos in serum-deprived cells is more unstable than nuclear c-Fos in cells cultured with serum (17) and (ii) cytoplasmic localization of c-Fos upon induction by STAT3 in the presence of inactivated Erk5 correlates with protein destabilization (14). Other possibilities, such as reloading of c-Fos with transcriptional co-activators or post-translational modifications in the cytoplasm or, alternatively, retrocontrol of c-fos mRNA translation by monomeric protein in excess will also have to be considered. Addressing this issue would require nuclear shuttling-deficient c-Fos mutants. Unfortunately, none of the many variants we have generated showed this property, which hampered this analysis.

Nuclear retention of c-Fos by c-Jun is primarily due to physical association via the LZ and neither to binding to DNA nor to indirect effects resulting from gene activation by c-Fos:c-Jun dimers. Moreover, our cell fractionation experiments indicate that inhibition of nuclear export is not due to simple masking of c-Fos NES but rather to the fact that c-Jun favors association with intranuclear components/structures. Further work will aim at identifying them. c-Fos shuttling is, however, not totally inhibited by an excess of c-Jun, whereas both c-Jun:c-Fos dimers stabilized in BiFC assays and the tethered c-Jun~c-Fos molecule, showed inefficient shuttling activity under the conditions used. Because AP-1 dimers constantly dissociate and reassociate in living cells (6, 38), these data suggest that basal shuttling of c-Fos in the presence of c-Jun concerns monomeric c-Fos and simply reflects de-dimerization of AP-1 dimers within the nucleus.

Interestingly, the various Jun proteins show differential ability to retain c-Fos in the nucleus, the effect of c-Jun being the strongest. Recent thermal denaturation studies of bZip dimers from the different Fos and Jun proteins have shown that c-Fos:JunB, c-Fos:JunD, JunB:JunB, and JunD:JunD dimers are much less stable than c-Fos:c-Jun and c-Jun:c-Jun ones (50). It is therefore worth noting that JunB and JunD shuttle more efficiently than c-Jun when transfected alone and retain c-Fos in the nucleus less efficiently than c-Jun in co-transfection assays. This further supports the idea that Fos:Jun dimer stability may be the primary factor determining c-Fos return rate into the cytoplasm.

In conclusion, we report here that monomeric c-Fos can undergo active nucleocytoplasmic shuttling. Nuclear export is, however, inhibited upon dimerization with Jun proteins, the consequence of which is to maintain functional AP-1 complexes within the nucleus. This situation is reminiscent of that of the ATF2 bZIP transcription factor whose nuclear retention by c-Jun has recently been reported (56). The degree of inhibition of c-Fos nuclear export depends on the Jun heterodimerization partner, which adds another layer of complexity to the finely tuned regulation of the family of AP-1 transcription complexes. At first approximation, inhibition efficiency correlates with the relative stabilities of the different Jun:c-Fos dimers, at

least as deduced from *in vitro* thermal denaturation studies of their bZip. As post-translational modifications can interfere with AP-1 dimer formation (6), an important question will, therefore, be to determine whether intracellular signaling can modulate c-Fos nucleocytoplasmic dynamics under physiological and/or pathological situations.

---

*Acknowledgments*—All imaging analyses were performed on the Montpellier Réseau Inter-Organismes imaging platform. We are indebted to Drs G. Bossis and H. Brooks for fruitful discussions and critical reading of the manuscript.

---

## REFERENCES

1. Eferl, R., and Wagner, E. F. (2003) *Nat. Rev. Cancer* **3**, 859–868
2. Hess, J., Angel, P., and Schorpp-Kistner, M. (2004) *J. Cell Sci.* **117**, 5965–5973
3. Milde-Langosch, K. (2005) *Eur. J. Cancer* **41**, 2449–2461
4. Shaulian, E., and Karin, M. (2002) *Nat. Cell Biol.* **4**, E131–E136
5. Young, M. R., and Colburn, N. H. (2006) *Gene (Amst.)* **379**, 1–11
6. Chinenov, Y., and Kerppola, T. K. (2001) *Oncogene* **20**, 2438–2452
7. Jariel-Encontre, I., and Piechaczyk, M. (2007) *Targeted Protein Data Base*, Current Biodata Ltd., London, in press
8. Salvat, C., Jariel-Encontre, I., Acquaviva, C., Omura, S., and Piechaczyk, M. (1998) *Oncogene* **17**, 327–337
9. Acquaviva, C., Brockly, F., Ferrara, P., Bossis, G., Salvat, C., Jariel-Encontre, I., and Piechaczyk, M. (2001) *Oncogene* **20**, 7563–7572
10. Ferrara, P., Andermarcher, E., Bossis, G., Acquaviva, C., Brockly, F., Jariel-Encontre, I., and Piechaczyk, M. (2003) *Oncogene* **22**, 1461–1474
11. Basbous, J., Jariel-Encontre, I., Gomard, T., Bossis, G., and Piechaczyk, M. (2007) *Biochimie (Paris)*, in press
12. Bossis, G., Ferrara, P., Acquaviva, C., Jariel-Encontre, I., and Piechaczyk, M. (2003) *Mol. Cell Biol.* **23**, 7425–7436
13. Basbous, J., Chalbos, D., Hipskind, R., Jariel-Encontre, I., and Piechaczyk, M. (2007) *Mol. Cell Biol.* **27**, 3936–3950
14. Sasaki, T., Kojima, H., Kishimoto, R., Ikeda, A., Kunimoto, H., and Nakajima, K. (2006) *Mol. Cell* **24**, 63–75
15. Murphy, L. O., and Blenis, J. (2006) *Trends Biochem. Sci.* **31**, 268–275
16. Bossis, G., Malnou, C. E., Farras, R., Andermarcher, E., Hipskind, R., Rodriguez, M., Schmidt, D., Muller, S., Jariel-Encontre, I., and Piechaczyk, M. (2005) *Mol. Cell Biol.* **25**, 6964–6979
17. Roux, P., Blanchard, J. M., Fernandez, A., Lamb, N., Jeanteur, P., and Piechaczyk, M. (1990) *Cell* **63**, 341–351
18. Tratner, I., and Verma, I. M. (1991) *Oncogene* **6**, 2049–2053
19. Campos, M. A., Kroon, E. G., Gentz, R., and Ferreira, P. C. (1999) *Cell Biol. Int.* **23**, 81–88
20. Forwood, J. K., Lam, M. H., and Jans, D. A. (2001) *Biochemistry* **40**, 5208–5217
21. Gorlich, D., and Kutay, U. (1999) *Annu. Rev. Cell Dev. Biol.* **15**, 607–660
22. Pemberton, L. F., and Paschal, B. M. (2005) *Traffic* **6**, 187–198
23. Arnold, M., Nath, A., Wohlwend, D., and Kehlenbach, R. H. (2006) *J. Biol. Chem.* **281**, 5492–5499
24. Vriza, S., Lemaître, J. M., Leibovici, M., Thierry, N., and Mechali, M. (1992) *Mol. Cell Biol.* **12**, 3548–3555
25. Bussolino, D. F., Guido, M. E., Gil, G. A., Borioli, G. A., Renner, M. L., Grabois, V. R., Conde, C. B., and Caputto, B. L. (2001) *FASEB J.* **15**, 556–568
26. Gil, G. A., Bussolino, D. F., Portal, M. M., Pecchio, A. A., Renner, M. L., Borioli, G. A., Guido, M. E., and Caputto, B. L. (2004) *Mol. Biol. Cell* **15**, 1881–1894
27. Tanos, T., Marinissen, M. J., Leskow, F. C., Hochbaum, D., Martinetto, H., Gutkind, J. S., and Coso, O. A. (2005) *J. Biol. Chem.* **280**, 18842–18852
28. Hu, C. D., Chinenov, Y., and Kerppola, T. K. (2002) *Mol. Cell* **9**, 789–798
29. Muller, S., Berger, M., Lehembre, F., Seeler, J. S., Haupt, Y., and Dejean, A. (2000) *J. Biol. Chem.* **275**, 13321–13329
30. Pfarr, C. M., Mechta, F., Spyrou, G., Lallemand, D., Carillo, S., and Yaniv, A.

- M. (1994) *Cell* **76**, 747–760
31. Lemercier, C., Brocard, M. P., Puvion-Dutilleul, F., Kao, H. Y., Albagli, O., and Khochbin, S. (2002) *J. Biol. Chem.* **277**, 22045–22052
  32. Bakiri, L., Matsuo, K., Wisniewska, M., Wagner, E. F., and Yaniv, M. (2002) *Mol. Cell. Biol.* **22**, 4952–4964
  33. Kudo, N., Wolff, B., Sekimoto, T., Schreiner, E. P., Yoneda, Y., Yanagida, M., Horinouchi, S., and Yoshida, M. (1998) *Exp. Cell Res.* **242**, 540–547
  34. Brusselbach, S., Mohle-Steinlein, U., Wang, Z. Q., Schreiber, M., Lucibello, F. C., Muller, R., and Wagner, E. F. (1995) *Oncogene* **10**, 79–86
  35. Sambrook, J., Fritsch, E. F., and Maniatis, T. (1989) in *Molecular Cloning* (Nolan, C., ed) pp. 16.32–16.33, Cold Spring Harbor Laboratory Press, Cold Spring Harbor, NY
  36. Roth, J., Dobbstein, M., Freedman, D. A., Shenk, T., and Levine, A. J. (1998) *EMBO J.* **17**, 554–564
  37. Wysocka, J., Reilly, P. T., and Herr, W. (2001) *Mol. Cell. Biol.* **21**, 3820–3829
  38. Kovary, K., and Bravo, R. (1991) *Mol. Cell. Biol.* **11**, 2451–2459
  39. Walther, R. F., Lamprecht, C., Ridsdale, A., Groulx, I., Lee, S., Lefebvre, Y. A., and Hache, R. J. (2003) *J. Biol. Chem.* **278**, 37858–37864
  40. Guttinger, S., Muhlhauser, P., Koller-Eichhorn, R., Brennecke, J., and Kutay, U. (2004) *Proc. Natl. Acad. Sci. U. S. A.* **101**, 2918–2923
  41. Rebane, A., Aab, A., and Steitz, J. A. (2004) *RNA (N. Y.)* **10**, 590–599
  42. Cartwright, P., and Helin, K. (2000) *Cell. Mol. Life Sci.* **57**, 1193–1206
  43. Fornerod, M., Ohno, M., Yoshida, M., and Mattaj, I. W. (1997) *Cell* **90**, 1051–1060
  44. Miska, E. A., Karlsson, C., Langley, E., Nielsen, S. J., Pines, J., and Kouzarides, T. (1999) *EMBO J.* **18**, 5099–5107
  45. Talcott, B., and Moore, M. S. (1999) *Trends Cell Biol.* **9**, 312–318
  46. Plafker, K., and Macara, I. G. (2000) *Mol. Cell. Biol.* **20**, 3510–3521
  47. Schuermann, M., Neuberger, M., Hunter, J. B., Jenuwein, T., Ryseck, R. P., Bravo, R., and Muller, R. (1989) *Cell* **56**, 507–516
  48. Ransone, L. J., Visvader, J., Wamsley, P., and Verma, I. M. (1990) *Proc. Natl. Acad. Sci. U. S. A.* **87**, 3806–3810
  49. Kovary, K., and Bravo, R. (1992) *Mol. Cell. Biol.* **12**, 5015–5023
  50. Mason, J. M., Schmitz, M. A., Muller, K. M., and Arndt, K. M. (2006) *Proc. Natl. Acad. Sci. U. S. A.* **103**, 8989–8994
  51. Chida, K., Nagamori, S., and Kuroki, T. (1999) *Cell. Mol. Life Sci.* **55**, 297–302
  52. Jakel, S., and Gorlich, D. (1998) *EMBO J.* **17**, 4491–4502
  53. Siomi, M. C., Eder, P. S., Kataoka, N., Wan, L., Liu, Q., and Dreyfuss, G. (1997) *J. Cell Biol.* **138**, 1181–1192
  54. Fan, X. C., and Steitz, J. A. (1998) *Proc. Natl. Acad. Sci. U. S. A.* **95**, 15293–15298
  55. Verhagen, J., Donnelly, M., and Elliott, G. (2006) *J. Virol.* **80**, 10021–10035
  56. Liu, H., Deng, X., Shyu, Y. J., Li, J. J., Taparowsky, E. J., and Hu, C. D. (2006) *EMBO J.* **25**, 1058–1069